

# A neural theory of circadian rhythms: Aschoff's rule in diurnal and nocturnal mammals

GAIL A. CARPENTER AND STEPHEN GROSSBERG

*Department of Mathematics, Northeastern University and Center for Adaptive Systems,  
Department of Mathematics, Boston University, Boston, Massachusetts 02215*

CARPENTER, GAIL A., AND STEPHEN GROSSBERG. A neural theory of circadian rhythms: Aschoff's rule in diurnal and nocturnal mammals. *Am. J. Physiol.* 247 (Regulatory Integrative Comp. Physiol. 16): R1067-R1082, 1984.—A neural model of the suprachiasmatic nuclei suggests how behavioral activity, rest, and circadian period depend on light intensity in diurnal and nocturnal mammals. These properties are traced to the action of light input (external zeitgeber) and an activity-mediated fatigue signal (internal zeitgeber) on the circadian pacemaker. Light enhances activity of the diurnal model and suppresses activity of the nocturnal model. Fatigue suppresses activity in both diurnal and nocturnal models. The asymmetrical action of light and fatigue in diurnal vs. nocturnal models explains the more consistent adherence of nocturnal mammals to Aschoff's rule, the consistent adherence of both diurnal and nocturnal mammals to the circadian rule, and the tendency of nocturnal mammals to lose circadian rhythmicity at lower light levels than diurnal mammals. The fatigue signal is related to the sleep process S of Borbély (*Hum. Neurobiol.* 1: 195-204, 1982.) and contributes to the stability of circadian period. Two predictions follow: diurnal mammals obey Aschoff's rule less consistently during a self-selected light-dark cycle than in constant light, and if light level is increased enough during sleep in diurnal mammals to compensate for eye closure, then Aschoff's rule will hold more consistently. The results are compared with those of Enright's model.

hypothalamus; suprachiasmatic nuclei; transmitter gate; instrumental behavior

## 1. Introduction: A Neural Model of Circadian System in Mammalian Suprachiasmatic Nuclei

A circadian pacemaker that helps to control the wake-sleep and activity-rest cycles of mammals has been identified in the suprachiasmatic nuclei (SCN) of the hypothalamus (17, 20, 28). A neural model of the SCN circadian system has recently been developed (5-7). This model was constructed from neural components that have also been used to model motivated behaviors, such as eating and drinking, that are controlled by other hypothalamic circuits (12, 13, 21). Thus our SCN model forms part of a larger theory of how hypothalamic circuits are specialized to control different types of motivated behaviors.

Perhaps for this reason our model has been able to quantitatively simulate a large body of circadian data. These data include split rhythms (16, 23, 25), several types of long-term aftereffects (3, 23, 24), phase response

curves to pulses of light in diurnal and nocturnal mammals, including the "dead zone" of phase resetting insensitivity during the subjective day of a nocturnal mammal (9, 10, 18, 26), SCN ablation studies (22), and suppression of the pacemaker by high light intensities (3, 11). Due to the fact that every process in the model has a physical interpretation, the model also suggests a number of anatomical, physiological, and pharmacological predictions to test its validity. Notable among these are predictions that test whether slowly varying transmitter gating actions form part of the SCN pacemaker. In model circuits controlling motivated behaviors such as eating and drinking, such slow gating processes have already been used to analyze a variety of abnormal behaviors, such as juvenile hyperactivity, Parkinsonism, hyperphagia, and simple schizophrenia (13, 14). If a slow gating action is verified in the SCN, it would provide a new basis for analyzing certain abnormalities of circadian rhythms and their effects on the motivational circuits that they modulate.

The present article analyzes Aschoff's rule and its exceptions and the circadian rule in diurnal and nocturnal mammals (1-3). This analysis is based on the same processes that have been used to explain all phenomena mentioned above. Each process can, in principle, be experimentally manipulated to test the analysis by causing determinate changes in Aschoff's rule. For example, we predict in section 10 that a diurnal mammal that obeys Aschoff's rule in a constant light environment will obey the rule less consistently at high light levels when given dark shelter or lights out during sleep. In section 15 we compare our analysis of Aschoff's rule with that of other models in the literature.

## 2. Aschoff's Rule, Circadian Rule, and Exceptions

Enright (11) describes Aschoff's rule and the circadian rule as follows:

1. "Aschoff's rule": For diurnal animals, the free-running period of a circadian activity rhythm usually decreases with increasing light intensity; the brighter the constant light, the faster the animal's "clock" runs. For nocturnal animals, the converse is usually observed: the free-running period of the rhythm increases with increasing light intensity.
2. The "circadian rule": For diurnal animals, brighter constant light prolongs daily wakefulness under free-running conditions, and also increases the level of arousal, as indicated by the intensity of locomotor activity. For nocturnal animals, the converse is true: brighter light usually shortens the duration of wakefulness and decreases the intensity of activity.

These rules hold when an animal is exposed to a constant light level at all times. The changes in period and activity level are functions of this light level as it is parametrically varied. Enright says that the described changes "usually" occur in diurnal and nocturnal animals. Actually there are pronounced differences in how universally these rules hold in diurnal and nocturnal mammals. For example, Aschoff (3) writes

For night-active species of mammals ... there is again an unambiguous picture: with the exception of the fruit bat, *Rousettus aegyptiacus*, all species lengthen  $\tau$  [period] as  $I_{LL}$  [light intensity] increases ... [but] a bimodal [decreasing-then-increasing] dependence of  $\tau$  on  $I_{LL}$  could be characteristic for at least some species of night-active mammals. Other than the quite uniform  $\tau$ -characteristics obtained from night-active mammals and day-active birds, the daytime species of mammals ... show large differences in the dependence of  $\tau$  on  $I_{LL}$ . A lengthening of  $\tau$  with increasing  $I_{LL}$  prevails, but four species shorten  $\tau$ , at least within certain ranges of intensities ....

Figure 1 describes characteristic data that illustrate Aschoff's rule.

Thus diurnal and nocturnal mammals are asymmetrical with respect to how frequently they violate Aschoff's rule. Nocturnal mammals obey the rule more consistently than diurnal mammals. When nocturnal mammals do not obey Aschoff's rule, a shortening of period usually occurs followed by a lengthening of period. Remarkably a similar shortening followed by a lengthening of period occurs in many diurnal mammals that do not obey Aschoff's rule (3), thereby sharpening the sense in which diurnal and nocturnal animals asymmetrically follow the rule.

### 3. Asymmetry of Fatigue and Light in Diurnal and Nocturnal Models

Our SCN model consists of a circadian pacemaker with a rhythm modulated by several types of signals. One signal is an external zeitgeber due to the action of light. Light input is defined to have opposite effects on the diurnal and nocturnal pacemaker. A second type of signal is a feedback signal to the pacemaker. This signal  $F$  is interpreted to be an index of the animal's metabolic activity as delivered to the pacemaker through the bloodstream. We call this  $F$  signal a fatigue signal because it tends to inhibit the activity-generating output signal in both the diurnal and the nocturnal models. Sources of the  $F$  signal are not necessarily restricted to metabolic consequences of overt motor activity. In its present form the model assumes that the signal builds up progressively as a function of its activity-generating output signal and exponentially decays during inactive intervals. The  $F$  signal is thus a type of activity-mediated internal zeitgeber. A third type of signal is also a feedback signal to the pacemaker. This signal buffers the pacemaker against adventitious light fluctuations, such as cloudy weather, yet enables it to react to pervasive lighting changes, such as seasonal changes. This feedback signal, which causes long-term aftereffects and the slow onset of split rhythms in the model (5, 7), will not be considered here.

We explain Aschoff's rule and its exceptions by analyzing the interactions between steady light inputs, the

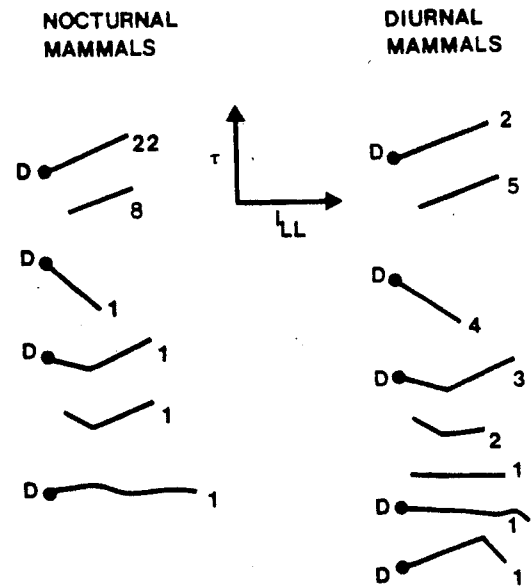


FIG. 1. Schematic graphs of  $\tau$  vs.  $I_{LL}$  summarized by Aschoff (3). Aschoff's review includes 34 experiments on 20 species of nocturnal mammals and 19 experiments on 16 species of diurnal mammals. Numbers, no. of Aschoff's graphs with similar shapes.  $D$  indicates that furthest left data point was computed from a free run in the dark. Most nocturnal  $\tau$  functions are monotone increasing. Diurnal  $\tau$  functions are more varied. See Aschoff (3) for references.

$F$  signal, and the pacemaker. In particular the predicted differences in the way diurnal and nocturnal activity durations and periods react to different levels of steady light will be traced to asymmetries in the action of light input and  $F$  signal on the diurnal and nocturnal pacemakers. Whereas both light and fatigue tend to inhibit activity-generating output of a nocturnal pacemaker, light excites and fatigue inhibits activity-generating output of a diurnal pacemaker. The more regular adherence of nocturnal mammals to Aschoff's rule will also be traced to this asymmetry.

In contrast the circadian rule is robustly obeyed in the model except in situations where long-term aftereffects predominate. The circadian rule states that an increase of steady light intensity stimulates activity in the diurnal animal and depresses activity in the nocturnal animal. We will explain why action of the light input tends to cause the circadian rule, despite action of the  $F$  signal, even in parameter ranges where the  $F$  signal plays a role in causing exceptions to Aschoff's rule.

### 4. A Connection Between Fatigue Signal and Sleep-Dependent Process $S$

Due to the importance of the  $F$  signal process in our explanation of Aschoff's rule, it is interesting to compare properties of this process with related concepts in the circadian literature. The sleep-dependent process  $S$  (4) is formally similar to our  $F$  process. If these two processes turn out to be the same, then manipulations of process  $S$  should affect period and activity levels in the manner predicted by our model.

Borbély (4) introduces process  $S$  to explain his data

about sleep regulation in humans. Process S is hypothesized to summate with the output of a circadian oscillator C that, in Borbély's measurements, covaries with the human temperature rhythm. The hypothesis that the sum of S and C signals regulates sleep is used to explain variations of sleep duration as a function of sleep deprivation and onset time.

Process S is assumed to progressively build up during an activity period and to exponentially decay within a few hours during sleep. These properties are also properties of the F signal. Our model can be combined with the sleep model of Borbély (4) in humans in two different ways. In one realization 1) the F signal accumulates during the waking state and exponentially decays on an ultradian time scale during sleep; 2) the F signal feeds back to the SCN pacemaker and depresses its activity-generating output; and 3) output from the SCN summates with a signal that covaries with the temperature rhythm. This sum controls onset and duration of sleep.

In the other realization 1 and 2 still hold. The large F signal shifts the base line, but not rhythmicity, of the SCN pacemaker. Output from the SCN controls the onset and duration of sleep and entrains the temperature rhythm.

### 5. Testing Existence of Fatigue Signal

The F signal plays a role in our SCN circadian model that is homologous to the role played by a satiety signal in our model of the hypothalamic eating circuit (12, 13). As in the case of the satiety signal it is far more difficult to characterize the biochemistry of a physiological signal than its existence and its behavioral properties. Our theory argues for the existence and properties of an F signal by demonstrating behavioral consequences of its presence or absence. Without this predictive linkage between behavior and physiology, it would be impossible to discover the chemical signals mediating fatigue feedback and its SCN receptors.

The present theory enables such biochemical tests to be made. For example, if a putative receptor is found, its elimination should cause either arrhythmicity or violations of Aschoff's rule in the manner predicted by the theory. Likewise if F signal receptors are found using this method, then putative chemical signals to the receptors can be tested by directly applying them to the receptor sites. Different courses of controlled chemical release lead to predictions about the dependence of circadian period on dosage.

The F signal also figures prominently in our explanation of split rhythms and long-term aftereffects (7). Destroying putative receptors or applying putative chemical signals leads to behavioral predictions about how split rhythms or long-term aftereffects will be altered. Finally the formal linkage between the F signal and Borbély's process S (4) enables electroencephalographic (EEG) measures to be used to test whether process S varies concurrently with the F signal in all experiments where Borbély's procedure can be used.

The net effect of our theory is thus to suggest many interdisciplinary experiments using biochemical, phys-

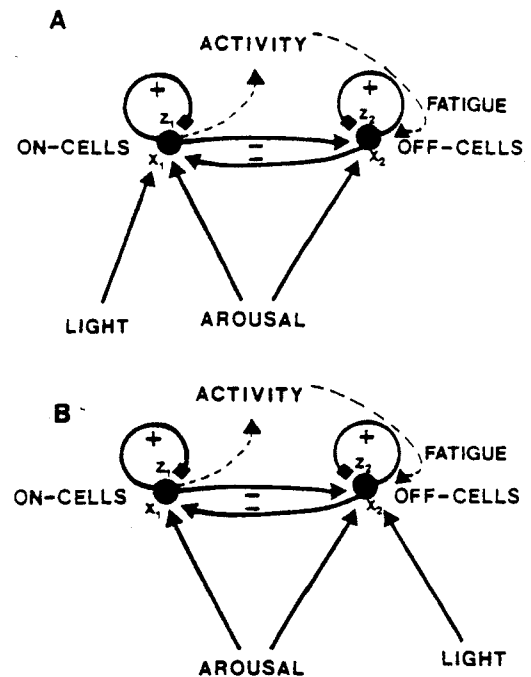


FIG. 2. Anatomy and physiology of diurnal (A) and nocturnal (B) gated pacemakers. Potential  $x_1$  of an on-cell (population) and potential  $x_2$  of an off-cell (population) obey Eqs. 1 and 2, respectively. Transmitter substance  $z_1$  gates the positive feedback signal  $f(x_1)$  from on-cells (population) to itself, and transmitter substance  $z_2$  gates positive feedback signal  $f(x_2)$  from off-cells (population) to itself.  $I$ , nonspecific arousal level, which excites on-cells and off-cells equally.  $F$  excites off-cells. Light input  $J(t)$  excites on-cells of diurnal model (A) and off-cells of nocturnal model (B). Transmitter  $z_1$  in Eq. 3 accumulates via term  $D(E - z_1)$  and is released at rate  $-Hf(x_1)z_1$ . A similar law governs  $z_2$  in Eq. 4.  $F$  signal in Eq. 5 builds up with behavioral activity via term  $h(x_1)$  and decays at a constant rate via term  $-KF$ . Many basic model properties persist in modified versions of Eqs. 1-5. Species-specific variations and future data may support particular versions without altering qualitative explanations of model properties.

iological, behavioral, and EEG methods to test for the existence and properties of the F signal.

### 6. Gated Pacemaker Model

The gated pacemaker model describes the dynamics of on-cell/off-cell pairs, called gated dipoles, in which on-cells and off-cells mutually inhibit one another. Populations of these gated dipoles are assumed to exist in each SCN. The following processes define the gated pacemaker dynamics that will be used in this article (Fig. 2): 1) slowly accumulating transmitter substances are depleted by gating the release of feedback signal; 2) feedback signals are organized as an on-center, of surround, or competitive, anatomy; 3) both on-cells and off-cells are tonically aroused; 4) light excites on-cells of a diurnal model and off-cells of a nocturnal model; 5) on-cells drive observable activity, such as wheel turning, in both diurnal and nocturnal models; 6) on-cell activity gives rise to an F signal that is fed back to the off-cells in both diurnal and nocturnal models. The signal is a time average of the on-cell output signal. The model equations for a nocturnal gated pacemaker are defined as follows:

$$dx_1/dt = -Ax_1 + (B - x_1)[I + f(x_1)z_1] - (x_1 + C)g(x_2) \quad (1n)$$

$$dx_2/dt = -Ax_2 + (B - x_2)[I + f(x_2)z_2 + F + J(t)] - (x_2 + C)g(x_1) \quad (2n)$$

$$dz_1/dt = D(E - z_1) - Hf(x_1)z_1 \quad (3)$$

$$dz_2/dt = D(E - z_2) - Hf(x_2)z_2 \quad (4)$$

$$dF/dt = -KF + h(x_1) \quad (5)$$

Variable  $x_1$  in Eq. 1n is the potential of an on-cell (population)  $v_1$ . Variable  $x_2$  in Eq. 2n is the potential of an off-cell (population)  $v_2$ . Both  $x_1$  and  $x_2$  obey membrane equations (15). In Eqs. 1n and 2n the parameter  $-A$  in terms  $-Ax_1$  and  $-Ax_2$  determines the fast decay rate of potentials  $x_1$  and  $x_2$ . Also in Eqs. 1n and 2n term  $I$  represents the arousal level that equally excites  $v_1$  and  $v_2$ . In Eq. 1n the transmitter substance  $z_1$  gates the nonnegative feedback signal  $f(x_1)$  from  $v_1$  to itself. Term  $f(x_1)z_1$  is proportional to the rate at which transmitter is released from the feedback pathway from  $v_1$  to itself, thereby reexciting  $x_1$ . Off-cells inhibit the on-cells via the nonnegative signal  $g(x_2)$  in term  $-(x_1 + C)g(x_2)$ . Equation 2n is the same as Eq. 1n, except that indexes 1 and 2 are interchanged and the light input  $J(t)$  excites  $v_2$ , not  $v_1$ , because Eqs. 1-5 represent a nocturnal model. Also the  $F$  signal excites  $v_2$  in both nocturnal and diurnal models.

Equations 3 and 4 define the transmitter processes  $z_1$  and  $z_2$ . In Eq. 3 the transmitter  $z_1$  accumulates to its maximal level  $E$  at a slow rate  $D$  via the term  $D(E - z_1)$ . This slow accumulation process is balanced by the release of  $z_1$  at rate  $Hf(x_1)z_1$ , leading to the excitation of  $x_1$  in Eq. 1n. A similar combination of slow accumulation and gated release defines the dynamics of transmitter  $z_2$  in Eq. 4.

The  $F$  signal in Eq. 5 is a time average of the on-cell output signal  $h(x_1)$ . The decay rate  $K$  of  $F$  is chosen to be slower than  $A$  in Eqs. 1n and 2n but faster than  $D$  in Eqs. 3 and 4. Whereas parameter  $D$  contributes to the model's circadian time scale, parameter  $K$  contributes to the model's ultradian time scale.

The diurnal gated pacemaker differs from the nocturnal pacemaker only in Eqs. 1d and 2d which define its on-cell and off-cell potentials.

$$dx_1/dt = -Ax_1 + (B - x_1)[I + f(x_1)z_1 + J(t)] - (x_1 + C)g(x_2) \quad (1d)$$

$$dx_2/dt = -Ax_2 + (B - x_2)[I + f(x_2)z_2 + F] - (x_2 + C)g(x_1) \quad (2d)$$

$$dz_1/dt = D(E - z_1) - Hf(x_1)z_1 \quad (3)$$

$$dz_2/dt = D(E - z_2) - Hf(x_2)z_2 \quad (4)$$

$$dF/dt = -KF + h(x_1) \quad (5)$$

Interpretation of the diurnal equations is similar to that of the nocturnal equations.

A comparison of the nocturnal pacemaker with the diurnal pacemaker leads to the following physiological

predictions. In nocturnal mammals there are SCN pacemaker cells at which the effects of a light pulse  $J$  and the fatigue signal  $F$  summate. These are the off-cells of Eq. 2n. In diurnal mammals a light pulse and the  $F$  signal are mutually inhibitory at all SCN pacemaker cells. Thus a light pulse  $J$  excites on-cells in Eq. 1d; the  $F$  signal excites off-cells in Eq. 2d, and on-cells and off-cells are mutually inhibitory. In both diurnal and nocturnal mammals a light pulse excites some SCN cells and inhibits other SCN cells. This is because light  $J$  excites either on-cells or off-cells, and these cell populations are mutually inhibitory. Also see section 16, which notes that light pulses may differentially excite both types of cells in some mammals.

### 7. Signal Functions, Activity Thresholds, and Attenuation of Light Input During Sleep

Models in Eqs. 1-5 are completely defined by a choice of the signal functions ( $f$ ,  $g$ ,  $h$ ), light input  $J(t)$ , and parameters. In all simulations the signal functions  $f(w)$  and  $g(w)$  in Eqs. 1-4 are chosen to be threshold-linear functions of activity  $w$

$$f(w) = \max(w, 0) \quad (6)$$

$$g(w) = \max(w, 0) \quad (7)$$

The signal function  $h(w)$  is defined in two steps. First, the on-cell output signal function  $h^*(w)$  is defined. Then we choose

$$h(w) = M \max[h^*(w) - h^*(N), 0] \quad (8)$$

Function  $h^*(w)$  is a sigmoid, or S-shaped, function of activity  $w$

$$h^*(w) = w^2/(P^2 + w^2) \quad (9)$$

In our numerical runs, only values of  $w$  where  $h(w)$  is approximately threshold-linear were used. Carpenter and Grossberg (6) analyze how pacemaker dynamics are altered by choosing different types of signal functions.

Physical interpretations of  $f$  and  $g$  have already been given. The definitions of  $h$  and  $h^*$  require further explanation. Function  $h^*[x_1(t)]$  is interpreted to be the on-cell output signal of the pacemaker. Behavioral activity is triggered when  $x_1(t)$  exceeds threshold  $N$ . The function  $h[x_1(t)]$  defined by Eq. 8 provides an index of behavioral activity. By Eq. 5 fatigue builds up at a rate proportional to behavioral activity. Activity ceases when  $x_1(t) \leq N$ . During such a time interval, fatigue decays at exponential rate  $K$ .

By so defining fatigue we provide a relatively simple description of the model. In more complex versions of the model, pacemaker output modulates the arousal level of motivational circuits (e.g., for eating, drinking, sex, exploratory activity). This arousal level helps to determine the sensitivity of these circuits to external and internal cues. The resultant behaviors have metabolic consequences that contribute to the fatigue signal (7, 13). This additional complexity has not been needed to qualitatively explain Aschoff's rule or the circadian rule.

Another factor that we consider herein concerns the distinction between overt activity (e.g., wheel turning),

wakeful rest, and sleep. In the circadian literature the total period ( $\tau$ ) is divided into time ( $\alpha$ ) during which the animal engages in overt activity and the remaining rest time ( $\rho$ ) (2). No distinction is made between wakeful rest and sleep despite a transitional time of wakeful rest before, after, and possibly during the overt activity cycle. This time of wakeful rest, during which the eyes are open but fatigue is decaying, plays a role in our analysis of Aschoff's rule because different light intensities can have differential effects on the durations of wakeful rest and sleep in the model.

To mathematically distinguish these three states, we assume as in Eq. 8 that overt activity takes place when

$$x_1(t) > N \quad (10)$$

A sleep threshold  $Q$  is also assumed to exist such that  $N > Q$ . When

$$Q < x_1(t) \leq N \quad (11)$$

the model is in a state of wakeful rest. When

$$x_1(t) \leq Q \quad (12)$$

the model is in a state of sleep. We define sleep in terms of its effects on the pacemaker. The main effect is that eye closure (or entering a dark nest) can attenuate the light input to the pacemaker. Letting  $L(t)$  be the light input that reaches the pacemaker when its "eyes" are open, we define the net light input in Eqs. 1d and 2n to be

$$J(t) = \begin{cases} L(t) & \text{if } x_1(t) > Q \\ \theta L(t) & \text{if } x_1(t) \leq Q \end{cases} \quad (13)$$

Parameter  $\theta$  is a light attenuation factor due to eye closure. Hence  $0 \leq \theta \leq 1$ . We systematically vary the size of  $\theta$  in our analysis. The fact that  $\theta$  is not always zero is implied by the ability of light pulses to phase shift a mammal's circadian rhythm while the mammal is asleep (6, 26).

Our definitions of wakeful rest and sleep are chosen for simplicity. In species for whom a separate temperature pacemaker helps control sleep onset, a more complex definition is needed to discuss situations wherein the SCN and temperature pacemakers become desynchronized (8, 30). Also, our definition of the feedback  $F$  signal assumes that no fatigue accumulates during wakeful rest. The simulations thus make the approximations that the  $F$  signal builds up much faster during overt activity than during wakeful rest and that all oscillators controlling sleep onset are approximately synchronized. In species that spend most waking hours actively exploring or consummating, the lack of fatigue buildup during wakeful rest causes no loss of generality. In other species an obvious extension of the model would postulate a smaller rate of fatigue buildup during wakeful rest than during overt activity. In any case the present hypotheses have proved sufficient to qualitatively explain Aschoff's rule and the circadian rule.

#### 8. Aschoff's Rule and its Exceptions: Numerical Studies

This section describes parametric numerical studies

that indicate the dynamic factors subserving Aschoff's rule and its exceptions in our model. The next section describes numerical studies of the circadian rule, and section 10 continues the analysis of how these numerical properties are generated. This analysis provides a dynamic explanation of how Aschoff's rule and the circadian rule depend on the physiological processes of our model. We pay particular attention to how the  $F$  signal and the amount of light attenuation that occurs during eye closure or lights out influences these rules. Analysis of the effects of light attenuation led, for example, to the prediction that diurnal mammals obey Aschoff's rule less consistently during a self-selected light-dark cycle than in constant light. As greater experimental control is achieved over the  $F$  signal, the analysis can be used to suggest behaviorally testable predictions about that process too. For example, we predict that nocturnal mammals which obey Aschoff's rule will either be arrhythmic (section 15) or violate Aschoff's rule if their  $F$  signal is blocked before it can modulate their SCN pacemaker. Given the formal similarity of the  $F$  signal to Borbély's sleep-dependent process  $S$  (section 15), these predictions may provide a way to experimentally probe process  $S$  using properties of Aschoff's rule and the circadian rule.

The numerical studies consider eight cases that arise from combining the following three alternatives in all possible ways: 1) nocturnal vs. diurnal, 2) no fatigue signal vs. large fatigue signal, and 3) no light attenuation by eye closure ( $\theta = 1$ ) vs. maximal light attenuation by eye closure ( $\theta = 0$ ).

Our main mechanistic insight about Aschoff's rule is that fatigue causes the rule to hold. The asymmetrical frequency with which the rule holds in diurnal vs. nocturnal mammals is traced to the asymmetrical manner in which light perturbs diurnal and nocturnal models with respect to site of action of fatigue (Fig. 2).

To start, consider the nocturnal and diurnal models with no fatigue ( $F = 0$ ) and no light attenuation ( $\theta = 1$ ). By Eqs. 1-5, the nocturnal and diurnal pacemaker models are symmetrical: off-cells in the nocturnal model play the role of on-cells in the diurnal model and conversely. Thus  $\tau$  of both models is the same. Consequently Aschoff's rule cannot occur in this case. It must depend on either fatigue, light attenuation, or both. In nocturnal and diurnal models on-cell output causes behavioral activity. The  $\alpha$  of the nocturnal model consequently varies in a complementary manner with respect to the  $\alpha$  of the diurnal model. This property exemplifies the fact that the circadian rule holds in our model in all eight cases.

Figure 3 summarizes how  $\tau$  varies with increasing steady light levels in the eight cases. In every case all parameters are held constant, other than the parameters controlling light attenuation ( $\theta$ ) and the amount of fatigue ( $M$  in Eq. 8). The fixed parameters are listed in Table 1. These parameters were chosen so that no single term in Eqs. 1-4 dominates any other term. A method for balancing terms in this way is described in Ref. 6, where it is shown that clock-like oscillations are generated within a wide numerical range of balanced parameters.

The parameters  $\theta$  and  $M$  were chosen to maximize the

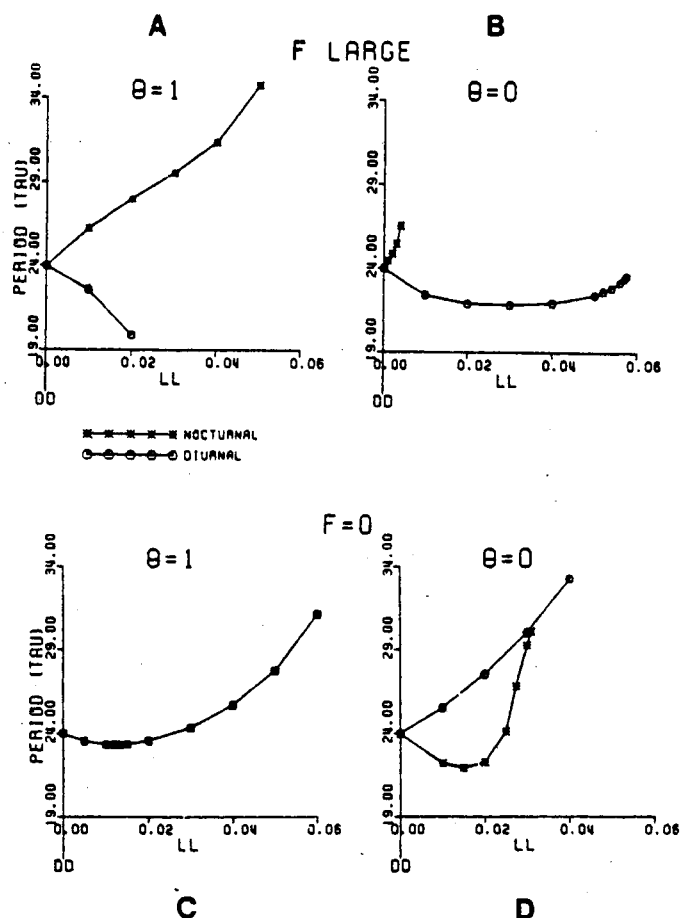


FIG. 3. Period  $\tau$  as function of light intensity LL; 8 curves correspond to 8 combinations of nocturnal vs. diurnal,  $\theta = 1$  vs.  $\theta = 0$ , and  $F$  large vs.  $F = 0$ . All model parameters are chosen as in Table 1. LL, linear function of logarithm of ambient light intensity. This transformation is assumed to occur in pathway from retinal receptors to suprachiasmatic nuclei. Choice  $A = 1$  in Table 1 fixes dimensionless time scale. For comparison we have transformed time scale so that in each case  $\tau = 24$  h in the dark. This is accomplished by multiplying dimensionless  $\tau$  of Eqs. 1-5 by 0.552 h (A, B) or by 0.305 h (C, D).

differences between small and large light attenuation and fatigue effects. In particular we chose  $\theta = 0$  in Fig. 3, B and D, to illustrate maximal light attenuation during sleep. We chose  $\theta = 1$  in Fig. 3, A and C, to illustrate no light attenuation during sleep. We chose  $M = 0$  and  $F(0) = 0$  in Fig. 3, C and D, to illustrate the case of zero fatigue. In Fig. 3, A and B,  $M$  was chosen to maximize the effects of fatigue. Very large  $M$  values cause such a large  $F$  signal that behavioral activity is suppressed almost as soon as it begins. In Fig. 3 comparing A with C and B with D shows the choice  $M = 0.1$  causes a significant effect of fatigue without preventing sustained bouts of behavioral activity from occurring.

We now consider Fig. 3 in detail. Each graph depicts period of the nocturnal model and the diurnal model as a function of parametric increases in steady light level (LL). Figure 3C describes the case of no light attenuation ( $\theta = 1$ ) and no fatigue ( $F = 0$ ). Because both nocturnal and diurnal models have the same period in this case, only one curve is shown. As a function of increasing LL,

this curve decreases before it increases. Thus the curve does not obey Aschoff's rule for either nocturnal or diurnal mammals. However, as shown in Fig. 1, there exists both nocturnal and diurnal mammals whose period changes in the manner of Fig. 3C as a function of LL.

In Fig. 3A no light attenuation during eye closure occurs, but there exists a significant  $F$  signal. The  $F$  signal causes distinct  $\tau$  values to occur in the nocturnal and diurnal models. Moreover, each graph of  $\tau$  vs. LL exhibits Aschoff's rule. In Fig. 3 the comparisons of A with C and B with D are the basis for our claim that fatigue is a primary factor in generating Aschoff's rule. This comparison also leads to the prediction that nocturnal mammals obeying Aschoff's rule will either be arrhythmic (section 15) or will violate Aschoff's rule if their  $F$  signal is blocked before it can modulate their SCN pacemaker.

Deviations from Aschoff's rule are explained by the joint action of fatigue and light attenuation due to eye closure. A comparison between Fig. 3, A and B, illustrates one of these deviations. In both figures fatigue feedback is effective. The figures differ only in how much light attenuation occurs during sleep. In Fig. 3B the nocturnal model continues to obey Aschoff's rule, whereas the diurnal model does not. This fact is a basis for our explanation of the greater tendency of nocturnal mammals to obey Aschoff's rule. Despite violation of Aschoff's rule by the diurnal model, the diurnal model's period curve is similar to curves generated by certain diurnal mammals (Fig. 1). The differential reactions of nocturnal and diurnal models to the interaction between light attenuation and fatigue reflects the asymmetrical sites of action of these factors in the nocturnal and diurnal pacemakers.

The rate-limiting role of fatigue in generating Aschoff's rule is again shown by comparing Fig. 3, B and D. In both cases light is significantly attenuated during eye closure. In Fig. 3D, however, no fatigue is registered at either pacemaker. At low light levels, curves generated by the nocturnal and diurnal models are opposite those one would expect from Aschoff's rule. Thus our model predicts that if a technique could be found to prevent registration of the hypothesized  $F$  signal by SCN off-cells, then the experimental animal should violate Aschoff's rule. The period  $\tau$  of the nocturnal model in Fig. 3D increases with LL at large values of LL. Thus in all the graphs in Fig. 3 the nocturnal model obeys Aschoff's rule, at least for large values of LL. This property also supports the idea that nocturnal mammals obey Aschoff's rule more consistently than diurnal mammals.

Due to the importance of the comparison between Fig. 3, A and B, we compare these curves with curves generated in response to a different choice of pacemaker parameters. Figure 4 shows the curves obtained when a parameters except the arousal level ( $I$  in Eqs. 1 and 2) are the same as in Table 1. To obtain Fig. 4 a low arousal level ( $I = 0.1$ ) was used. All qualitative properties of Fig. 3, A and B, are preserved in Fig. 4, A and B, respectively. Aschoff's rule again holds in Fig. 4A.  $T$  curves in Fig. 4B look as if their abscissas have been stretched at small values of LL. The effect causes,

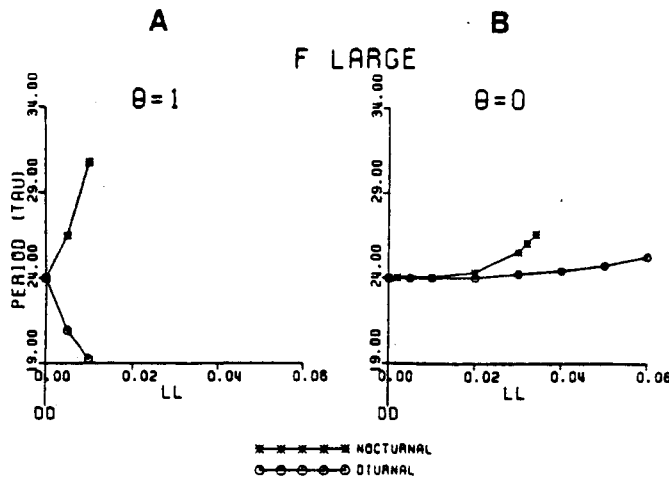


FIG. 4. Period  $\tau$  as function of light intensity LL. The 4 curves correspond to 4 combinations of nocturnal vs. diurnal and  $\theta = 1$  vs.  $\theta = 0$  when  $F$  is large. Arousal level  $I = 0.1$ . All other parameters are chosen as in Table 1. By multiplying dimensionless  $\tau$  values of Eqs. 1-5 by scaling factor 0.472 h,  $\tau$  in the dark is fixed at 24 h.

TABLE 1. Parameter values

Parameter	Value	Interpretation
A	1	$x_1$ decay rate
B	5	maximal $x_1$
C	0.5	minimal $x_1$
D	0.01	$z_1$ accumulation rate (slow)
E	0.4	maximal $z_1$
H	0.02	$z_1$ release rate
I	0.13	arousal
K	0.17	$F$ decay rate
N	0.72	activity threshold
Q	0.67	sleep threshold
P	1	$x_1$ value where on-cell output is half-maximal
M	$\begin{cases} 0 \\ 0.1 \end{cases}$	$F = 0$ $F$ large
$\theta$	$\begin{cases} 1 \\ 0 \end{cases}$	no light attenuation during sleep complete light attenuation during sleep

example, the period curve of the nocturnal model in Fig. 4B to increase more slowly as a function of LL than in Fig. 3B. In Figs. 3B and 4B the nocturnal model loses circadian rhythmicity at a lower light level than the diurnal model. Thus the model reflects Aschoff's observation (3): "Among the mammals, an intensity of 100 lx. is surpassed by 37% of noctactive species, and by 71% of the dayactive species."

### 9. Circadian Rule: Numerical Studies

In contrast to Aschoff's rule, the circadian rule holds for both nocturnal and diurnal model in all eight cases. Figure 5 summarizes illustrative numerical results by plotting  $\alpha$  (duration of behavioral activity) as a function of LL. We define  $\alpha$  in the model as the total amount of time during each cycle when

$$x_1(t) > N \quad (10)$$

as in section 7. In all cases  $\alpha$  increases with LL in the diurnal model and decreases with LL in the nocturnal

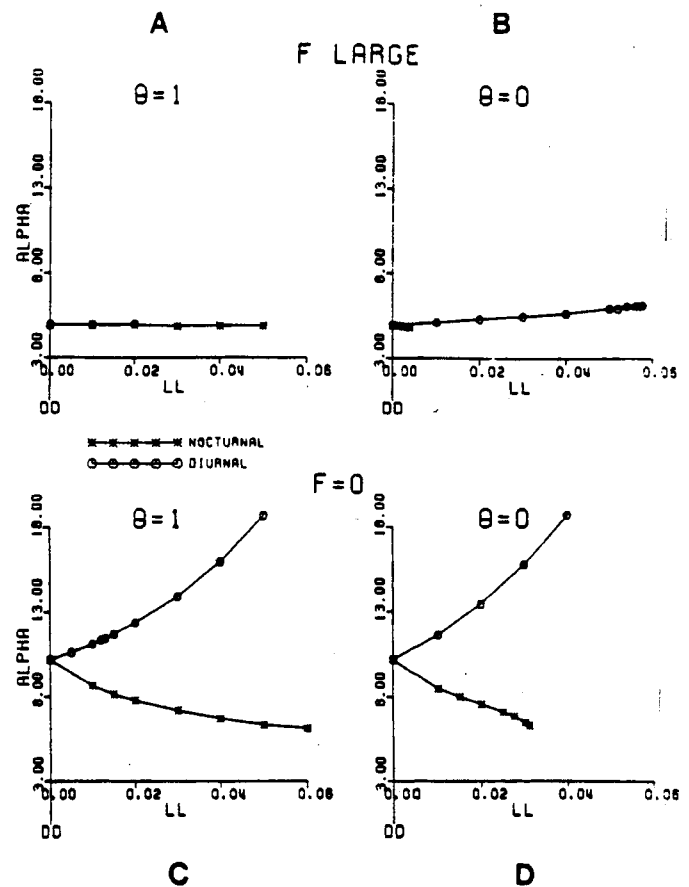


FIG. 5. Length  $\alpha$  of activity interval as a function of light intensity LL. Systems in A-D correspond to systems in Fig. 3, A-D, respectively.

model, as essentially always occurs in the mammalian data. The circadian rule is primarily due to the fact that light excites on-cells in the diurnal model and off-cells in the nocturnal model, whereas in both cases on-cell output supports behavioral activity.

Why do light attenuation and fatigue not cause frequent exceptions to the circadian rule as they do to Aschoff's rule? This issue will be more extensively discussed in sections 12 and 13, but some intuitive comments can immediately be made. Fatigue is a feedback signal that is contingent upon on-cell activity. Whenever fatigue becomes strong enough to attenuate on-cell activity while the animal is active, it also undermines its own source of activation. An analysis of wakeful rest and sleep shows how fatigue causes its different effects on  $\alpha$  and  $\tau$ . Light attenuation occurs only when the animal is asleep. Hence it has little effect on  $\alpha$  and the circadian rule, as can be seen by comparing Fig. 5A with 5B and Fig. 5C with 5D.

By comparing Figs. 3 and 5, numerical plots of  $\rho$  (duration of wakeful rest plus sleep) as a function of LL are obtained. Figure 6 shows that  $\rho$  is not always a monotonic function of LL despite the fact that  $\alpha$  is always a monotonic function of LL. The comparison between Figs. 5 and 6 provides one of many examples showing that the relationship between activity and subsequent rest-sleep is far from simple.



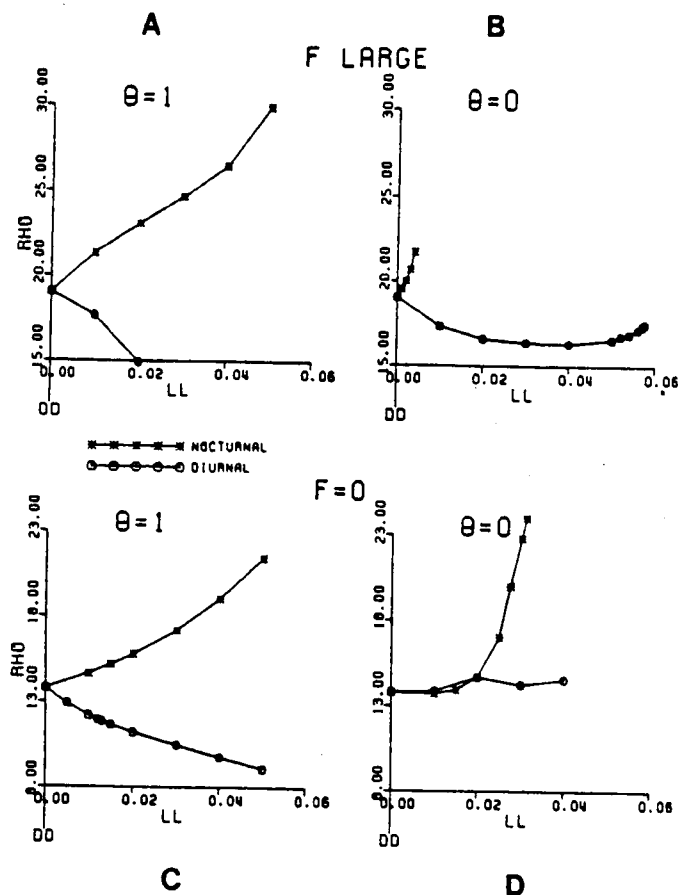


FIG. 6. Length  $\rho$  of rest interval as function of light intensity LL. Systems A-D correspond to systems in Fig. 3, A-D, respectively.

#### 10. Light Attenuation and Self-Selected Light-Dark Cycles in Diurnal Mammals: A Prediction

The importance of the light attenuation factor  $\theta$  is shown by experiments on diurnal mammals which contrast the  $\tau$  that is found under steady light conditions with the  $\tau$  that occurs when the mammal can eliminate light before going to sleep. Our analysis leads to some predictions within this paradigm.

As reported by Aschoff (3) "... lengthenings of  $\tau$  due to self-selected light-dark cycles have been observed in the Rhesus monkey, *Macaca mulatta*, [31], in the squirrel monkey, *Saimiri sciureus*, (Tokura and Aschoff, unpubl.) and in man [29]." Wever (30) reports numerous experiments on man in which  $\tau$  is longer during self-selected light-dark cycles than during constant illumination.

We predict that a diurnal mammal which self-selects light-dark cycles will, at sufficiently high illuminations, tend to violate Aschoff's rule more than the same mammal kept in continuous light at these illumination levels. We also predict that if light level is increased enough during sleep in diurnal mammals to compensate for eye closure, then Aschoff's rule will tend to hold more consistently.

As pointed out by Wever (30), a self-selected light-dark cycle is experienced, to some extent, by any animal

that shuts its eyes during sleep. In the model, normal eye closure in a lighted room corresponds to a value of  $\theta$  between 0 and 1. A self-selected light-dark cycle is identified with the case  $\theta = 0$ . The case  $\theta = 1$ , in contrast, corresponds to an animal which is sensitive to light even when its eyes are closed and has no dark hiding place.

Figures 3 and 4 indicate that a lengthening of  $\tau$  occurs in the diurnal gated pacemaker with complete light attenuation during sleep. In all cases and at all light levels,  $\tau$  is lengthened when  $\theta = 0$  (right columns) compared with when  $\theta = 1$  (left columns). This is because a model animal asleep in the dark ( $\theta = 0$ ) must wait for the internal pacemaker dynamics to cause awakening. However, a model animal asleep in the light ( $\theta > 0$ ) has the joint action of both arousal ( $I$ ) and light input ( $J = \theta L$ ) in Eqs. 1d and 13 working to hasten the onset of the next activity cycle. Thus  $\rho$  is shorter when  $\theta$  is positive than when  $\theta = 0$ , as in Fig. 6 (diurnal). Consequently  $\tau$  is also shorter when  $\theta$  is positive than when  $\theta = 0$ , as in Figs. 3 and 4 (diurnal).

Finally, comparisons between A and B in both Fig. 3 and Fig. 4 suggest the following prediction. When  $F$  is large and  $\theta = 1$  (Figs. 3A and 4A), Aschoff's rule holds: diurnal  $\tau$  decreases as LL increases. In contrast, when  $\theta = 0$ , the graph of diurnal  $\tau$  values first decreases and then increases. The model thus predicts that a diurnal mammal which obeys Aschoff's rule in a constant light environment will obey the rule less consistently at high light levels when given dark shelter or lights out during sleep and will obey Aschoff's rule more consistently if light level is increased during sleep.

#### 11. Stability of $\tau$ : Clock-Like Properties of Gated Pacemaker

Almost by definition a circadian pacemaker must keep approximately accurate time despite the intrusion of a fluctuating chemical or electrical environment. The basic gated pacemaker, without fatigue, is clock-like in the dark (6). In particular the transmitter accumulation rate ( $D$ ) in Eqs. 3 and 4 determines the approximate period of the pacemaker in the dark, except near the limits where circadian rhythmicity breaks down. Once  $D$  is fixed the other parameters such as arousal level ( $I$ ) have comparatively little effect on  $\tau$ .

Except at extreme parameter values this stability of  $\tau$  is maintained by the joint action of fatigue and light attenuation (Fig. 4B). Section 13 will analyze the following properties in detail. If the diurnal pacemaker receives a light input at the on-cells the subsequent increased on-cell activity causes a larger  $F$  signal to the off-cells, and the new balance between light and fatigue keeps  $\alpha$  close to its dark value. If the nocturnal pacemaker receives a light input at the off-cells, the subsequent decreased on-cell activity causes a smaller  $F$  signal to the off-cells: the sum of light input plus fatigue at the off-cells is balanced, and  $\alpha$  is again preserved. During sleep in both diurnal and nocturnal models, light attenuation implies that  $\rho$  is relatively unaffected by the ambient light level. Thus the sum  $\tau = \alpha + \rho$  is kept approximately constant and independent of the light levels.



## 12. Analysis of Aschoff's Rule

We will now analyze the factors that generate curves of the form shown in Figs. 3-6. Of the eight cases (nocturnal vs. diurnal,  $F = 0$  vs.  $F$  large, and  $\theta = 0$  vs.  $\theta = 1$ ), some can be easily explained by using qualitative arguments. These cases will be treated in the present section. The more difficult cases are discussed in sections 13 and 14.

**A. Basic pacemaker:  $F = 0$  and  $\theta = 1$ .** Consider Fig. 3C. In this case neither fatigue feedback nor light attenuation due to eye closure occurs, so both diurnal and nocturnal models generate the same  $\tau$  as a function of LL. Consider a diurnal model for definiteness. How can we explain the effect of a parametric increase in steady light level on such a model?

By Eq. 1d the light input  $J(t)$  directly excites on-cells. As a first approximation, an increase in  $J$  tends to shift the graph of  $x_1(t)$  upward. Figure 7A depicts an upward shift of the graph  $x_1(t)$  generated by the model in the dark. This upward shift idealizes the effect of a parametric increase in LL. Figure 7B compares the graph of  $x_1(t)$  generated in the dark with the graph of  $x_1(t)$  generated by a positive level of LL.

In Fig. 7A the graph of  $x_1(t)$  is compared with the threshold  $N$  at which the model becomes active. The activity period  $\alpha$  is the total time when

$$x_1(t) > N \quad (10)$$

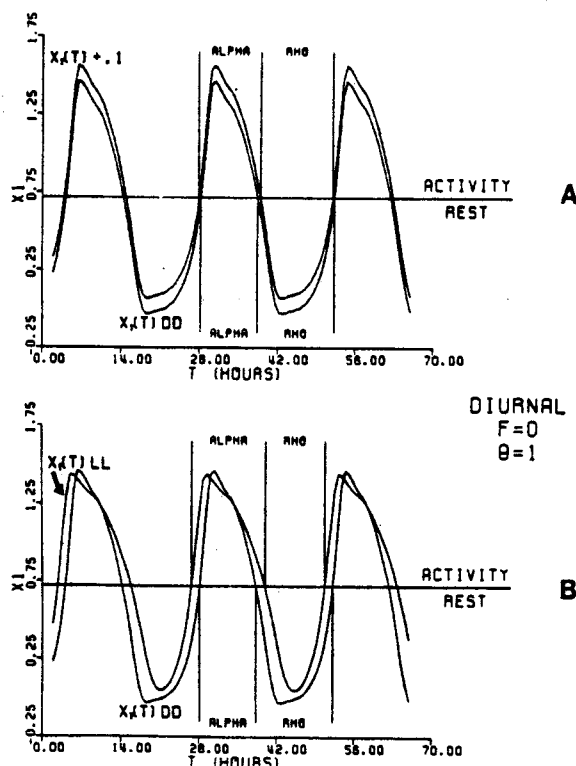


FIG. 7. Comparison of on-cell potential in light with an upward shift of on-cell potential in the dark. Diurnal on-cell potentials  $x_1(t)$  are plotted for case  $F = 0$  and  $\theta = 1$ , as in Figs. 3C, 5C, and 6C. All parameters are chosen as in Table 1. A plots  $x_1(t)$  in the dark, and same curve shifted upward by 0.1. B plots  $x_1(t)$  in the dark and  $x_1(t)$  when LL = 0.026. In all 4 curves  $\tau = 24$  h.

during one cycle. In Fig. 7A the increment  $\Delta\alpha$  in  $\alpha$  caused by an upward shift in the graph of  $x_1(t)$  is compensated by an equal decrement  $\Delta\rho$  in  $\rho$ . Consequently  $\tau$  does not change as LL increases if the only effect of LL is to cause an upward shift in the graph of  $x_1(t)$ . Figure 7B shows that the upward shift described by Fig. 7A is approximately valid. At the light level chosen for Fig. 7B,  $\Delta\alpha$  exactly balances  $\Delta\rho$  so that  $\tau$  in LL equals  $\tau$  in DD. The shift approximation is valid at low and moderate light levels (Fig. 3C) but begins to break down at high light levels. Section 14 explains why this happens.

**B. Aschoff's rule is due to fatigue:  $F$  large and  $\theta = 1$ .** Our explanation of Aschoff's rule depends on the fact that fatigue can cause a relatively large change in the approximate balance between  $\Delta\alpha$  and  $\Delta\rho$ . A comparison between Fig. 5, A and C, ( $\alpha$ ) and between Fig. 6, A and C, ( $\rho$ ) illustrates this property of the model. In Fig. 5A the graphs of  $\alpha$  as a function of LL are relatively flat; in Fig. 5C the graph of the diurnal  $\alpha$  rises sharply, and the graph of the nocturnal  $\alpha$  falls sharply as LL increases. In contrast the graph of nocturnal  $\rho$  in Fig. 6A is similar to that of the nocturnal  $\rho$  in Fig. 6C, and the diurnal  $\rho$  graphs are also similar. The effect of fatigue on the balance between  $\alpha$  and  $\rho$  gives Aschoff's rule in Figs. 3A and 4A. We now consider how fatigue causes large deviations in this approximate balance of  $\Delta\alpha$  and  $\Delta\rho$ .

Consider the diurnal model depicted in Fig. 3A. In this model the  $F$  signal becomes large during activity, but no light attenuation occurs during sleep. We assume that fatigue decays with a time scale that is shorter than the duration of  $\rho$  in the no-fatigue case (Fig. 3C). Under these circumstances light activates on-cell activity that in turn causes a build up of fatigue. Fatigue excites the off-cells that inhibit the on-cells, thereby tending to shut down the on-cell activity. Fatigue then tends to shorten, or clip, the time intervals when  $x_1(t)$  is large. Parameter  $\alpha$  is hereby significantly decreased by the action of fatigue. In contrast, after on-cell activity is reduced and rest or sleep begins, the  $F$  signal is no longer activated by the on-cells. Fatigue exponentially decays with a time scale that is shorter than the duration of  $\rho$  in the no-fatigue case. Thus the  $F$  signal has significantly decayed before off-cell activity would otherwise spontaneously decay. Fatigue consequently has little effect on  $\rho$ .

The net effect of fatigue in this case is to cause a significant decrease of  $\alpha$  relative to the no-fatigue case and a small change in  $\rho$  relative to the no-fatigue case. In all, a decrease in  $\tau$  is caused. As LL is parametrically increased, these effects of fatigue also increase. Thus a decrease of  $\tau$  as a function of LL is predicted in the diurnal model of Fig. 3A. A comparison of  $\alpha$  values for the diurnal models, as described in Fig. 5, A and C, shows that a large  $F$  signal can almost eliminate the increase in  $\alpha$  that would otherwise be caused by light. A similar comparison of Fig. 6, A and C, shows that a large  $F$  signal has little effect on  $\rho$  as a function of LL.

A similar argument applies to the nocturnal model in Fig. 3A. The main difference with the diurnal model is that light and fatigue both activate off-cells. In the absence of fatigue, LL increases  $\rho$  and decreases  $\alpha$  (Figs. 5C and 6C). In the nocturnal model with fatigue, a parametric increase in LL causes a parametric decrease

in on-cell activity that in turn causes a parametric decrease in fatigue. This parametric decrease in fatigue tends to disinhibit parametrically on-cell activity. Consequently fatigue tends to compensate for the direct effect of LL on the decrease in  $\alpha$ . Thus  $\alpha$  decreases more slowly with fatigue than without fatigue as LL increases. The increase of  $\rho$  with LL accompanied by the attenuated decrease in  $\alpha$  with LL predicts that  $\tau$  increases with LL in this nocturnal model. A comparison of the nocturnal models described in Figs. 5, A and C, shows that a large F signal can almost eliminate the decrease in  $\alpha$  that would otherwise be caused by light. A similar comparison of Fig. 6, A and C, shows that a large F signal has little effect upon  $\rho$  as a function of LL.

C. *Light attenuation during sleep:  $\theta = 0$ .* We now consider some of the main effects that are due to light attenuation during sleep. Two general properties guide this discussion: 1) because light is not attenuated when the model is active, light attenuation has little effect on  $\alpha$  in Fig. 5, B and D, compared with Fig. 5, A and C, respectively, in which no light attenuation occurs; 2) the effects of light attenuation on  $\rho$  are more subtle. Parameter  $\rho$  is the sum of the durations of wakeful rest and sleep within one cycle. Light attenuation occurs only during the sleep component of  $\rho$ . Figure 8 describes the effects of a shift in the curve of  $x_1(t)$  on the duration of wakeful rest. The shift in Fig. 8 causes approximately no change in this duration. This is not always true, and section 13 will investigate those cases in which the duration of wakeful rest changes significantly as LL increases. Where this approximation holds, we can conclude that the duration of wakeful rest changes relatively little as a function of LL. The main differential effects of  $\theta = 0$  vs.  $\theta = 1$  on  $\rho$  occur during the sleep interval.

If  $\theta = 0$ , then no light is registered during sleep. Let us assume that the model is in approximately the same state whenever  $x_1(t)$  reaches the sleep threshold  $Q$ , as in Eq. 12. Because no light is registered during sleep, the duration of sleep will then be approximately constant as LL increases.

Because  $\rho$  is the sum of wakeful rest and sleep durations,  $\rho$  is approximately constant as LL increases, if the

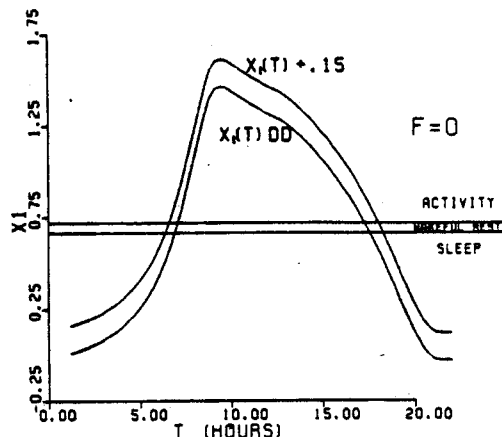


FIG. 8. Graph  $x_1(t)$  in the dark is compared with same curve shifted up by 0.15. Durations of 2 brief wakeful rest periods are little affected by such a shift. All parameters are chosen as in Table 1.

approximations we have made are valid for diurnal models. A comparison of Fig. 6, B and D, with Fig. 6, A and C, illustrates the extent to which this property holds especially for diurnal models.

D. *Exceptions to Aschoff's rule:  $F = 0$  and  $\theta = 0$ .* Let us apply these approximations to the diurnal model in Fig. 3D. This diurnal model differs from the diurnal model in Fig. 3C only because it attenuates light during sleep. In the diurnal model of Fig. 3C an increase of LL causes an increase of  $\alpha$  and a decrease of  $\rho$ . By the above argument the increase of  $\alpha$  is little affected by light attenuation, but the decrease of  $\rho$  (Fig. 6C) is eliminated in the diurnal model with  $\theta = 0$  (Fig. 6D). The net effect is an increase of  $\tau$  as a function of LL, which is observed (Fig. 3D).

Similarly, to understand the nocturnal model of Fig. 3D, we compare it with the nocturnal model of Fig. 3C. In this latter model ( $F = 0$  and  $\theta = 1$ ), an increase of LL causes a decrease of  $\alpha$  and an increase of  $\rho$ . This decrease of  $\alpha$  is little affected by switching from case  $\theta = 1$  to  $\theta = 0$ , because light attenuation during sleep has little effect on wakeful activity (Fig. 5D). In contrast, switching from case  $\theta = 1$  to  $\theta = 0$  has a large effect on  $\rho$ . In  $\theta = 0$ , changes in light intensity tend not to influence  $\rho$ . Figure 6D shows that this tendency is valid at low and moderate light levels. Section 14 explains why  $\rho$  increases with LL at large light levels.

E. *Difficult cases.* The preceding analysis does not answer the following questions. 1) When F is large and  $\theta = 0$ , why does the nocturnal model obey Aschoff's rule while the diurnal model generates a nonmonotonic (Fig. 3B)? 2) In the absence of fatigue, why does the nocturnal  $\tau$  always increase at high light levels (Fig. 3, C and D)? Answers to these questions require a more detailed analysis of the dynamics of Eqs. 1-5 than that which was used to explain the other cases. This fine analysis is described in sections 13 and 14.

### 13. Analysis of Joint Action of Fatigue and Light Attenuation on Circadian Period

To answer the first question we need to consider more closely the asymmetrical action of fatigue and light attenuation of the diurnal and nocturnal models. No argument has yet studied how these factors alter dynamics of the transmitter gates  $z_1$  and  $z_2$  through time. Now we do so.

First we will discuss the diurnal model of Fig. 3B. This model differs from the diurnal model of Fig. 3A only because it attenuates light during sleep. We can therefore use the same reasoning as in Fig. 3A to conclude that in Fig. 3B and 5B is relatively insensitive of LL. All our analysis will be devoted to showing why  $\rho$  (Fig. 6B), and hence  $\tau$ , first decreases and then increases as a function of LL. We consider the decreasing and the increasing portions of the  $\rho$  curve separately.

A. *Basic pacemaker in the dark.* To begin this analysis we need to study how  $x_1$  and  $x_2$  are switched on and off. For simplicity, we first consider the pacemaker when the light input is zero ( $J = 0$ ) and fatigue is zero ( $F = 0$ ). This basic pacemaker is analyzed in detail in Carpenter

and Grossberg (6). The pacemaker equations for the gated pacemaker in the dark with no fatigue are

$$dx_1/dt = -Ax_1 + (B - x_1)[I + f(x_1)z_1] - (x_1 + C)g(x_2) \quad (14)$$

$$dx_2/dt = -Ax_2 + (B - x_2)[I + f(x_2)z_2] - (x_2 + C)g(x_1) \quad (15)$$

$$dz_1/dt = D(E - z_1) - Hf(x_1)z_1 \quad (3)$$

$$dz_2/dt = D(E - z_2) - Hf(x_2)z_2 \quad (4)$$

Suppose that this system begins with  $x_1$  large and  $x_2$  small, but with both transmitters fully accumulated, so that by Eqs. 3 and 4  $z_1 \cong E$  and  $z_2 \cong E$ . At first,  $x_1$  maintains its advantage over  $x_2$  as follows. Because  $x_1$  is large and  $z_1 \cong E$ , the feedback signal from the on-cell (population)  $v_1$  to itself is large, as is the negative feedback signal  $g(x_1)$  from  $v_1$  to the off-cell (population)  $v_2$ . Because  $f(x_1)$  is large, however,  $z_1$  is slowly depleted at the rate  $-Hf(x_1)z_1$  by Eq. 3. As a result the gated signal  $f(x_1)z_1$  gradually becomes small despite the fact that  $x_1$  remains large.

During this time  $x_2$  and its feedback signal  $f(x_2)$  remain small. Thus the transmitter release rate  $-Hf(x_2)z_2$  in Eq. 4 also remains small, and  $z_2$  remains large as  $z_1$  is gradually depleted. As a result of these changes the positive feedback term

$$(B - x_1)[I + f(x_1)z_1] \quad (16)$$

in Eq. 14 diminishes relative to the positive feedback term

$$(B - x_2)[I + f(x_2)z_2] \quad (17)$$

in Eq. 15. Because  $f(w) = \max(w, 0)$  by Eq. 6 the feedback functions

$$H_z(w) = (B - w)[I + f(w)z] \quad (18)$$

have the form depicted in Fig. 9 at different values of  $z$ . If  $x_2$  is near zero then  $H_{z_2}(x_2) \cong BI$  given any value of  $z_2$ ,  $0 \leq z_2 \leq E$ . In contrast, if  $x_1$  is large  $H_{z_1}(x_1) > BI$  for  $z_1 \cong E$ , whereas  $H_{z_1}(x_1) < BI$  for  $z_1 \cong 0$ . Thus as  $z_1$  is depleted, the relative sizes of Eqs. 16 and 18 can reverse, even while  $x_1$  is still large.

Due to the relatively large decrease in Eq. 16,  $x_1$  itself begins to decrease, as does  $g(x_1)$  in Eq. 15. The positive term (Eq. 17) in Eq. 15 can therefore begin to overcome the negative feedback term

$$-(x_2 + C)g(x_1) \quad (19)$$

in Eq. 15, and  $x_2$  begins to grow. At first the growth of  $x_2$  does not depend on the size of  $z_2$ , because if  $x_2$  is small then  $H_{z_2}(x_2) \cong BI$  no matter how  $z$  is chosen. As  $x_2$  begins to increase, however, the continued increase of  $x_2$  depends critically on the fact that  $z_2$  is large, since  $H_E(x_2)$  is an increasing function of  $x_2$ , whereas  $H_0(x_2)$  is a decreasing function of  $x_2$  (Fig. 9). Because  $z_2$  is large when  $x_2$  begins to grow, a switch in the relative sizes of  $x_1$  and  $x_2$  occurs. As  $x_2$  becomes large, it suppresses  $x_1$  via the large negative feedback signal  $g(x_2)$  in Eq. 14. Now  $x_2$  has the advantage, and the competitive cycle starts to

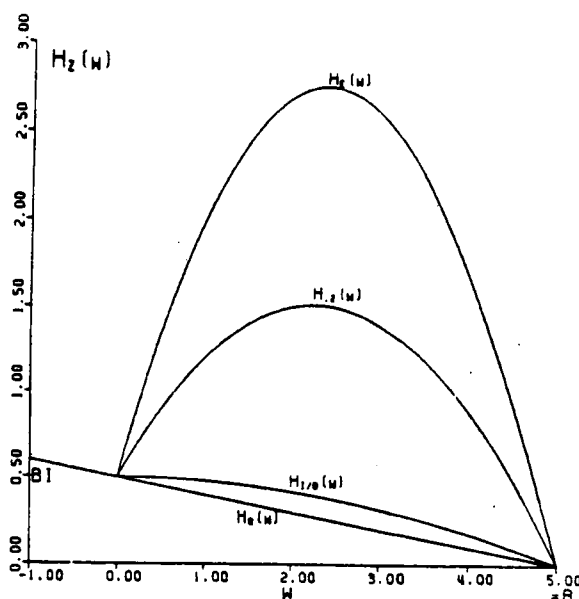


FIG. 9. Positive feedback function  $H_z(w)$  in Eq. 18 plotted as function of  $w$  at several values of parameter  $z$ . When  $z < I/B$ ,  $H_z(w)$  is a decreasing function of  $w$ . When  $z > I/B$ ,  $H_z(w)$  has a local maximum between  $w = 0$  and  $w = B$ . In the plots,  $B = 5$ ,  $E = 0.4$ ,  $I = 0.1$ , and  $f(w) = \max(w, 0)$ .

repeat itself as  $z_2$  is depleted and  $z_1$  is replenished.

**B. Diurnal model with  $F$  large and  $\theta = 0$ .** To understand the diurnal model of Figs. 3B and 4B, the influences of fatigue and light attenuation on the pacemaker must be considered. To study the influence of these factors on  $\rho$ , we consider the phase of the circadian cycle when  $x_2$  has just won the competition with  $x_1$ . Due to the earlier large values of  $x_1$ , the  $F$  signal is large at this transition by Eq. 5. As  $x_1$  decreases below the sleep threshold  $Q$  in Eq. 12, the light input  $J(t)$  shuts off, because  $\theta = 0$  in Eq. 13. Consequently throughout the sleep interval, only the arousal input  $I$  occurs in Eq. 1d to help  $x_1$  compete with  $x_2$ , and  $x_1$  obeys Eq. 14 of a basic pacemaker in the dark.

In contrast, at the beginning of wakeful rest and sleep,  $x_2$  receives a large  $F$  signal. This signal acts like an excitatory input that increases the asymptote of  $x_2$  relative to the values attained by the pacemaker Eq. 15 without fatigue. Furthermore, increased LL causes increased levels of fatigue, and hence larger  $x_2$  values, early in sleep. A larger  $x_2$  function causes a smaller  $z_2$  function by Eq. 4. Figure 10 shows how the graph of  $z_2$  is depressed by the action of light, via the  $F$  signal in Eq. 2d.

During wakeful rest and sleep  $h(x_1) = 0$  by Eq. 8. Thus  $F$  decays at the exponential rate  $K$  during this interval, as in Eq. 5. Because  $F$  decays on an ultradian time scale, it becomes approximately zero significantly before the end of the sleep interval. The transmitter gate  $z_2$  fluctuates on a slower time scale, however, so the depression of  $z_2$  caused by  $F$  persists for a longer time.

The transition between increasing values of  $x_1$  and decreasing values of  $x_2$  begins while the model is asleep. During this time potential  $x_1$  is activated only by arousal  $I$ . Potential  $x_2$  is no longer directly influenced by  $F$ ,

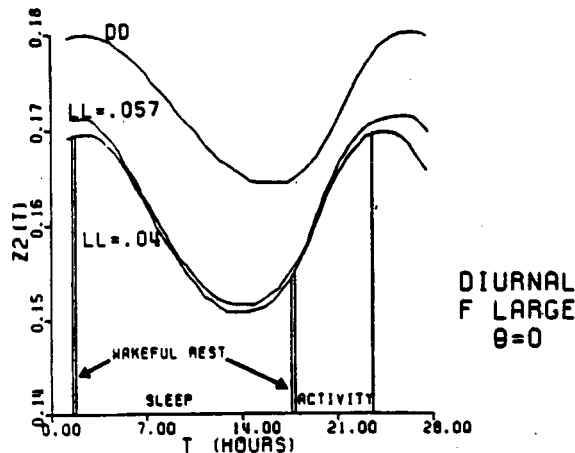


FIG. 10. Graphs of  $z_2(t)$  at 3 light levels (LL): LL = 0, 0.04, and 0.057. All parameters are chosen as in Table 1 for diurnal model with  $F$  large and  $\theta = 0$ . Graph of  $z_2(t)$  when LL = 0.04 lies below graphs of  $z_2(t)$  when LL = 0 and 0.057. Similarly in Fig. 3B,  $\tau$  is smaller when LL = 0.04 than when LL = 0 and 0.057. See text for explanation of covariance of  $z_2$  and  $\tau$ . Intervals of sleep, wakeful rest, and activity for case LL = 0.04 are bound by vertical lines.

although  $z_2$  is still smaller than it would have been in the dark. The transition toward wakeful rest is controlled by the pacemaker equations without fatigue in the dark, namely Eqs. 3, 4, 14, and 15. For wakeful rest to begin,  $z_2$  must first decay to a value such that the arousal  $I$  of  $x_1$  can begin the switch between  $x_2$  and  $x_1$ . In other words, the value to which  $z_2$  must decay is relatively insensitive to the prior light intensity  $J$  and the prior size of the  $F$  signal. Because  $z_2$  was already driven to smaller values by  $F$ , however, the remaining decrement in  $z_2$  needed for the transition to begin takes less time to occur than in the absence of  $F$ . This property explains the decrease of  $\rho$  with increasing LL in Fig. 5B.

The increase of  $\rho$  at large values of LL is due to an increase in the durations of both wakeful rest (following activity) and sleep. The increased duration of wakeful rest is explained as follows. As light input  $J$  is parametrically increased, the potential  $x_1$  remains within a fixed interval  $-C \leq x_1 \leq B$ . By Eq. 5 the  $F$  signal averages  $h(x_1)$  at a constant rate  $K$ . Thus at relatively large values of  $J$ , the maximal size of  $F$  does not grow linearly with  $J$ . In particular, at the threshold  $N$  between activity and wakeful rest, the value  $F_N(J)$  of  $F$  does not grow linearly with  $J$ . As soon as wakeful rest begins  $h(x_1) = 0$ , and  $F$  decays exponentially at the constant rate  $K$  from its initial value  $F_N(J)$ . Thus the size of the decaying signal  $F$  that excites  $x_2$  does not keep up with the size of  $J$  that excites  $x_1$ . It therefore takes longer for  $x_1$  to decay from the activity threshold  $N$  to the sleep threshold  $Q$ .

The duration of sleep increases at large  $J$  values for the following reason. Due to the longer duration of wakeful rest at large values of  $J$ , the value  $F_Q(J)$  of fatigue at the onset of sleep is a decreasing function of  $J$  at these  $J$  values. As in the explanation of why sleep duration decreases at small values of  $J$ , a smaller value of  $F_Q(J)$  implies a larger value of  $z_2$  at the onset of sleep (Fig. 10). Consequently it takes longer for  $z_2$  to decay to the point where a switch from large  $x_2$  values to large  $x_1$  values can

begin. The duration of sleep thus increases with  $J$  at large values of  $J$ .

**C. Nocturnal model with  $F$  large and  $\theta = 0$ .** We now explain why  $\tau$  increases with LL in the nocturnal model of Figs. 3B and 4B wherein both large  $F$  signals and light attenuation occur. This increase in  $\tau$  is due to the increase of  $\rho$  with LL (Fig. 6B), because  $\alpha$  is fairly constant as a function of LL (Fig. 5B). Most of this increase in  $\rho$  is due to an increase in the duration of sleep. The duration of wakeful rest is relatively constant and brief.

The reasons for these properties follow. In the nocturnal model light input  $J$  excites the off-cell potential  $x_2$ . In the absence of fatigue, increasing LL would imply decreasing  $\alpha$ , as in Fig. 5D. The decrease in  $x_1$  that would otherwise cause a decrease in  $\alpha$  also causes a decrease in  $F$ . Consequently  $\alpha$  is approximately constant as LL increases in Fig. 5B (section 9). Despite the relative insensitivity of  $\alpha$  to LL in this case, the size of  $x_1$  during the active period depends on LL. Early in the active period a larger light input  $J$  (Eq. 2n) causes a larger  $x_2$ , hence a smaller  $x_1$  (Fig. 11). The smaller  $x_1$  graph gradually gives

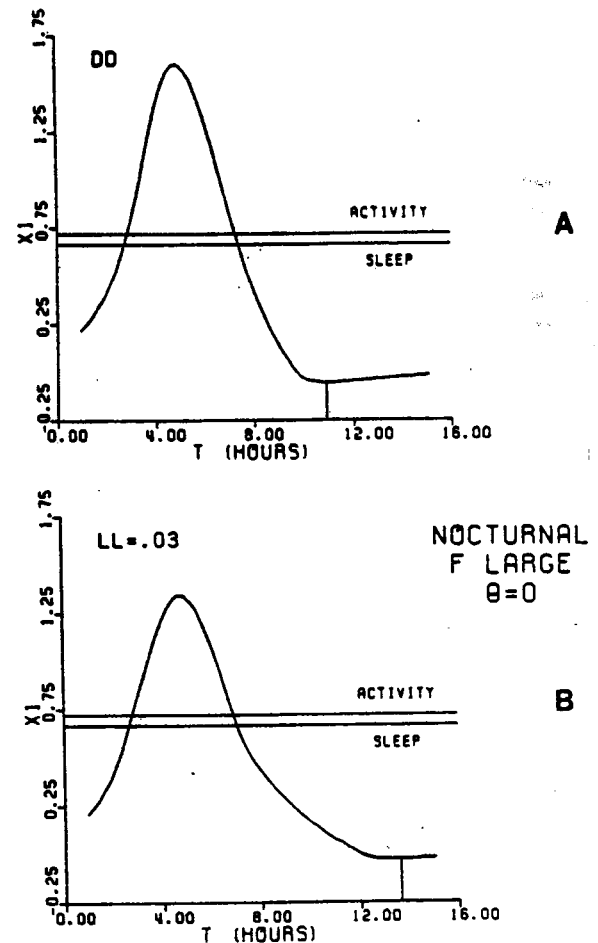


FIG. 11. Increase in initial segment of sleep interval when light level (LL) is increased. This increase occurs in nocturnal model with  $F$  large and  $\theta = 0$ . In A, LL = 0. On-cell potential  $x_1(t)$  has a maximum value of 1.6 and a minimum value that occurs 3.5 h after sleep onset. In B LL = 0.03. Then  $x_1(t)$  has a maximum value of 1.35 and a minimum value that occurs 6 h after sleep onset. In both A and B, arousal level  $I = 0.1$ , as in Fig. 4.

rise to a smaller  $F$ . By the end of the activity period, a larger  $J$  is compensated by a smaller  $F$ . Thus the sum  $J + F$  in Eq. 2n is relatively independent of  $J$  by the end to the activity period.

At the onset of sleep  $J$  shuts off because  $\theta = 0$ . Because at sleep onset  $J + F$  in LL is about the same size as  $F$  alone in DD,  $F$  in LL is smaller than  $F$  in DD. The smaller  $F$  input to  $x_2$  causes  $x_2$  to increase more slowly and hence causes  $x_1$  to decrease more slowly in the light than in the dark. In LL then,  $x_1$  takes longer to reach its minimum (Fig. 11). The increase in  $\rho$  caused by this lengthening of the early sleep interval accounts for the increase of  $\tau$  with increasing light levels in the nocturnal model with large  $F$  and  $\theta = 0$ .

We have now answered the first question of section 12E.

#### 14. Analysis of Pacemaker Without Fatigue

The second question of section 12E addresses the problem of why nocturnal models without fatigue have increasing  $\tau$  values at high light intensities, as do all the nocturnal mammals in Aschoff's survey (3). Sections 12 and 13 have already shown why, with a large  $F$  signal, nocturnal  $\tau$  values increase monotonically as light increases. To answer the question about nocturnal models without fatigue, we again need to investigate the dynamics of transmitters  $z_1$  and  $z_2$ .

A. *Nocturnal pacemaker with  $F = 0$  and  $\theta = 0$ .* We first consider why  $\rho$ , and hence  $\tau$ , increases with LL at large light intensities in the nocturnal model with  $F = 0$  and  $\theta = 0$  (Figs. 3D and 6D). We will explain how bright light forces the nocturnal model to terminate its activity cycle before the pacemaker, in the absence of light, would have induced sleep. A period of restless oscillation between waking and sleeping follows the active phase until sleep is finally induced. This restless time below the threshold of overt activity accounts for the increase in  $\rho$  and  $\tau$  at high light intensities.

Explanation of these properties follow. During the active phase when  $x_1 > N$ , the on-cell potential  $x_1$  is larger than the off-cell potential  $x_2$ . A large light input  $J$  to the off-cell  $v_2$  boosts  $x_2$  to larger values than  $x_2$  would have reached in the dark. The inhibitory term

$$-(x_1 + C)g(x_2) \quad (20)$$

in Eq. 1n is also boosted when  $x_2$  is boosted and thereby hastens termination of the active phase.

In the absence of the large light input  $J$ , the active phase would have terminated only after the transmitter  $z_1$  had been depleted (section 13A). In the presence of this light input, termination occurs without the full depletion of  $z_1$ . Due to its slow rate of change,  $z_1$  is still larger at the onset of sleep than it would have been in the absence of light input. Also at the onset of sleep the large light input  $J$  suddenly shuts off. At this time the "restless oscillation" between sleep and wakeful rest is triggered for the following reasons.

When  $J$  shuts off,  $x_2$  loses its major source of excitatory input. The still large  $z_1$  then enables  $x_1$  to increase. As soon as  $x_1$  recrosses the sleep threshold  $Q$ , however, the

light input  $J$  turns on, and  $x_2$  begins to grow again. Consequently  $x_1$  is forced below  $Q$ , and  $J$  shuts off. This oscillation of  $x_1$  around  $Q$  continues while  $z_1$  slowly depletes. Finally  $z_1$  depletes to a value that prevents  $x_1$  from recovering in the dark, and a sustained sleep epoch ensues. The time during which  $x_1(t)$  oscillates about the sleep threshold  $Q$  is the main factor causing the sharp increase in  $\rho$  at high LL values that is seen in Fig. 6D.

The diurnal pacemaker exhibits no large change in  $\rho$  at high light levels (Fig. 6D). This difference between the diurnal and nocturnal models is explained as follows. In the diurnal model bright light enhances and prolongs behavioral activity by its direct input to the on-cell (Eq. 1d). The increased  $x_1$  values in bright light lead to additional depletion of  $z_1$  by the onset of sleep. This extra depletion of  $z_1$  accelerates the rise of  $x_2$  after the light input shuts off and thus shortens  $\rho$  somewhat (Fig. 6D).

The restless oscillation that causes a large change in  $\rho$  in the nocturnal model does not occur because the light cooperates with  $x_1$  to cause  $z_1$  depletion. In particular, at the onset of sleep  $z_1$  is smaller due to prior light than it would have been in the dark. The offset of light and the smaller  $z_1$  value at sleep onset cause a sustained sleep epoch to ensue. The duration of this sleep epoch is not prolonged by the smaller  $z_1$  value because the depletion of  $z_2$  triggers the onset of activity. Only after  $x_2$  decreases and  $x_1$  increases due to  $z_2$  depletion does the accumulated  $z_1$  value maintain large  $x_1$  values (section 13).

B. *Diurnal and nocturnal pacemakers with  $F = 0$  and  $\theta = 1$ .* As noted in section 12A the nocturnal and diurnal pacemakers are symmetrical if  $F = 0$  and  $\theta = 1$ . They therefore have identical  $\tau$  graphs (Fig. 3C). We also remarked that small constant light inputs tend to cause upward (diurnal) or downward (nocturnal) shifts in the graph of  $x_1$  (Fig. 7). Because such shifts leave  $\tau$  unchanged, the graph of  $\tau$  is relatively flat at low light levels (Fig. 3C).

We will now consider the diurnal model at the high constant light levels where  $\alpha$  grows rapidly with LL (Fig. 5C). We will show that an increase in LL elongates the plateau of  $x_1$  values during the active phase, thereby increasing  $\alpha$ .

In the dark a switch from large  $x_1$  to small  $x_1$  occurs when the on-cell positive feedback term

$$(B - x_1)[I + f(x_1)z_1] \quad (16)$$

diminishes relative to the off-cell positive feedback term

$$(B - x_2)[I + f(x_2)z_2] \quad (17)$$

Recall that Eq. 17 approximately equals  $BI$  before the switch. A constant light input of intensity  $J$  changes the on-cell positive feedback term (Eq. 16) to

$$(B - x_1)[I + f(x_1)z_1 + J] \quad (21)$$

The off-cell positive feedback term (Eq. 17) is unchanged.

To see why the switch from large  $x_1$  to small  $x_1$  is progressively delayed by larger values of  $J$ , consider times shortly after  $x_1$  becomes large. During these times the gradual decay of  $z_1$  causes Eq. 21 to diminish relative to Eq. 17, which approximately equals  $BI$ . For a switch to

small  $x_1$  values to occur,  $z_1$  must decay to values in the presence of a large  $J$  smaller than in the dark. Other parameters being equal, an increase in  $J$  prolongs the time necessary for  $z_1$  to decay the requisite amount to cause a switch. While  $z_1$  is decaying,  $x_1$  remains at a large value. The graph of  $x_1$  thus develops a progressively larger plateau as  $J$  is parametrically increased (Fig. 7B).

### 15. Comparison with Other Models

Most other models of circadian rhythms do not explain exceptions to Aschoff's rule. The model of Enright (11) is a notable exception. This section compares our results with those of Enright so as to clarify the implications of both models.

Enright's model is a quasi-neural model in the following sense. The model's intuitive basis derives from a formal description of pacemaker neurons with activation thresholds that decay during each recovery phase. These pacemakers are not dynamically defined. Enright defines his model in terms of stochastic variables such as the average duration of the discharge phase, the average duration of the recovery phase, and the amount by which internal feedback shortens the average recovery phase. This stochastic description enables Enright to analyze consequences of his main hypothesis. This hypothesis states that circadian properties are due to entrainment of many individual circadian pacemakers with individual circadian properties only roughly specified.

The main elements of the Enright model are depicted in Fig. 12. A large population of endogenously active pacers  $P_1, P_2, \dots, P_n$  are assumed to have approximately circadian periods. The output of each pacer is a binary function that equals one when the pacer is "active" and zero when the pacer is "inactive." Each pacer excites the discriminator  $D$ . The total input to the discriminator at any time equals the number of active pacers.

The discriminator fires an output signal only if the total input exceeds a threshold  $\theta$ . The output of  $D$  is also a binary function. When  $D$  fires, it generates a feedback signal that equally excites every pacer. The model does not describe how this feedback signal alters the individual pacers. Instead Enright (11) makes the statistical hypothesis that the feedback signal decreases the average duration of recovery of the pacer population. The net effect of the feedback signal is to synchronize the pacer

population. It does this by speeding up the recovery of inactive pacers so that all pacers become active  $\pi$  synchronously during the next activity cycle.

The only effect of light in the model is to change discriminator threshold  $\theta$ . In a diurnal model  $\theta$  decreases as LL increases. In a nocturnal model  $\theta$  increases as LL increases. Thus a diurnal model with increasing LL is indistinguishable from a nocturnal model with decreasing LL. If the family of all nocturnal models and family of all diurnal models are chosen to exhaust same parameter space, then nocturnal and diurnal properties are completely symmetrical.

Using these hypotheses Enright (11) simulates Aschoff's rule and the circadian rule in his nocturnal diurnal models. Once these rules are simulated for diurnal model they automatically follow for the nocturnal model by symmetry. The decrease of  $\tau$  with increasing LL in Enright's diurnal model follows from the assumption that as light level increases fewer pacers need to be active for  $D$  to fire. The feedback signal from  $D$  to pacers thus acts earlier during the aggregate buildup of pacer activity and thereby shortens the mean duration of the pacers' recovery phases. Because duration of a pacer's active phase is assumed to be directly proportional to the previous recovery phase,  $\tau$  is shortened as LL increases.

At extreme parameter values, Enright's model violates Aschoff's rule (11). These exceptions occur with 1) each pacer's active phase is a large fraction of previous recovery phase and 2) discriminator feedback causes a large reduction ( $\epsilon$ ) in mean recovery time of the pacers. "In this circumstance, the accelerating influence of  $\epsilon$ , during the latter portion of the activity time extends through the entire inactive phase of the cycle and therefore affects many of those pacers which would ordinarily be involved in the subsequent onset of feedback." In other words when  $\theta$  is small, several pacers are able to fire twice during a single discriminator cycle, this brings about both a lengthening of  $\tau$  and a lengthening of  $\alpha$ . In this case Aschoff's rule is violated with the circadian rule still holds.

The circadian rule holds in Enright's model because first, each pacer is assumed to be active a fixed proportion of the time. This proportion is assumed not to change due to discriminator feedback or light input. Thus with a decrease of  $\theta$  causes a decrease in the average recovery duration of all pacers, the average active duration decreases. Each individual pacer therefore tends to violate the circadian rule. By a second assumption, however the fixed ratio of active time to recovery time in each pacer maintains the time average of the total input to the discriminator integrated over at least one period, at a constant level. Thus at smaller values of  $\theta$ ,  $D$  is active for a larger fraction of the cycle, so  $\alpha$  tends to be larger.

The formal nature of the hypotheses leading to the explanations of Aschoff's rule and the circadian rule is not problematic. These formal hypotheses could in principle later be instantiated by neural mechanisms. There are serious difficulties in explaining mammalian data concerning the symmetry between nocturnal and diurnal models in Enright's explanation of Aschoff's rule and

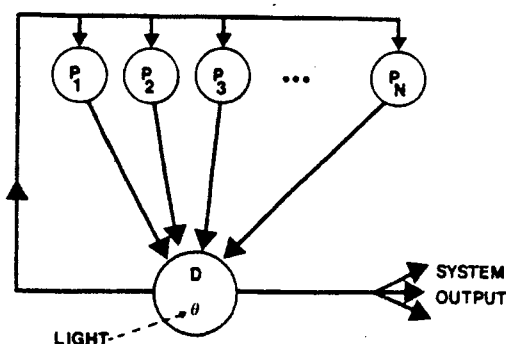


FIG. 12. Schematic representation of Enright's coupled stochastic system.

consistency with which Enright's model obeys Aschoff's rule in diurnal models. These formal properties are compatible with Enright's goal of considering all vertebrates, not only mammals. In particular, as Aschoff (3) points out, "The data on birds . . . show an unambiguous picture for the day active species . . . with increasing  $I_{LL}$ ,  $\tau$  shortens above a certain threshold-intensity, whereas towards lower values of  $I_{LL}$ ,  $\tau$  seems to level off." Thus diurnal birds tend to obey Aschoff's rule, following Enright's interpretation of his discriminator  $D$  as a model of the pineal organ in birds. However, Aschoff (3) then goes on to say "other than the quite uniform  $\tau$ -characteristics obtained from nocturnal mammals and day-active birds, the dayactive species of mammals . . . show large differences in the dependence of  $\tau$  on  $I_{LL}$ ." Thus diurnal mammals do not consistently obey Aschoff's rule, following the absence of any mention of the mammalian SCN in Enright's discussion.

Enright formally explains a nonmonotonic  $\tau$  by assuming that the model acts like a diurnal model at small values of  $LL$  and like a nocturnal model at large values of  $LL$ . Other difficulties of the Enright model concern its inability to explain phase response curves to brief light pulses, long-term aftereffects, and split rhythms (11) without making additional hypotheses for each phenomenon.

Points of comparison exist between the gated pacemaker model and the Enright model. The most important comparison concerns the possible role of asynchronous pacers and of synchronizing feedback in Enright's explanation of Aschoff's rule and the circadian rule. Our model also possesses individual pacers and a synchronizing feedback signal. The individual pacers are gated pacemakers, located in the SCN or, by extension, in other parts of the brain. The feedback signal is the  $F$  signal that, like the Enright discriminator, is activated by output from all pacers and acts as an internal zeitgeber, keeping the pacemakers in phase. In contrast to the Enright model we have shown that Aschoff's rule and the circadian rule can be explained even if the dispersions of individual pacer periods and phases are small relative to the time scales of the  $F$  signal and slow gating processes. An extension of our argument to the case in which individual pacers have significantly different periods and phases during free run can be given. These gated pace-

makers would still be synchronized by the feedback  $F$  signal. At present, however, our argument suggests that these properties are unnecessary to explain Aschoff's rule. Direct measurement of individual periods and phases of SCN pacemaker cells during free run would clarify this issue.

#### 16. Switching Between Diurnal and Nocturnal Properties

Other analogs also exist between the two models. In Enright (11) a switch between diurnal and nocturnal properties in a single model can be effected by changing the rule whereby discriminator threshold  $\theta$  is modified by light. In our model diurnal vs. nocturnal properties are due to the excitation of on-cells vs. off-cells by light. Both nocturnal and diurnal properties can be generated by specifying the light intensity ranges where on-cells or off-cells will be excited. For example, Enright (11) reviews the Martinez (19) data about the rhesus monkey that may be compatible with such a possibility. Whatever the interpretation of these data, a mechanism for switching between diurnal and nocturnal properties at different intensity levels is easily imagined in our model: let the light-activated off-cell input pathway have a higher threshold than the light-activated on-cell input pathway, and let the off-cell pathway vigorously inhibit the on-cell pathway when it is activated.

Some mammals, such as the vole, switch from nocturnal to diurnal properties as the seasons change (27). This change can be conceptualized in our model by a switch from activation of the on-cell input pathway to activation of the off-cell input pathway due to a seasonally modulated gating action on these pathways. The slow-gain control process we use to explain the slow onset of split rhythms and of long-term aftereffects is sensitive to seasonal variations in lighting level (5, 7). Either this process or a formally analogous process could, in principle, be the source of the gating signals that control seasonal switches between nocturnal and diurnal properties in a gated pacemaker model.

This study was supported in part by Air Force Office of Scientific Research Grant 82-0148 and National Science Foundation Grant MCS-82-07778.

Received 1 September 1983; accepted in final form 6 July 1984.

#### REFERENCES

1. ASCHOFF, J. Tierische Periodik unter dem Einfluss von Zeitgebern. *Z. Tierpsychol.* 15: 1-30, 1958.
2. ASCHOFF, J. Exogenous and endogenous components in circadian rhythms. *Cold Spring Harbor Symp. Quant. Biol.* 25: 11-28, 1960.
3. ASCHOFF, J. Influences of internal and external factors on the period measured in constant conditions. *Z. Tierpsychol.* 49: 225-249, 1979.
4. BORBÉLY, A. A. A two process model of sleep regulation. *Hum. Neurobiol.* 1: 195-204, 1982.
5. CARPENTER, G. A., AND S. GROSSBERG. Dynamic models of neural systems: propagated signals, photoreceptor transduction, and circadian rhythms. In: *Oscillations in Mathematical Biology*, edited by J. P. E. Hodgson. New York: Springer-Verlag, 1983, p. 102-196.
6. CARPENTER, G. A., AND S. GROSSBERG. A neural theory of circadian rhythms: the gated pacemaker. *Biol. Cybernetics* 48: 35-59, 1983.
7. CARPENTER, G. A., AND S. GROSSBERG. A neural theory of circadian rhythms: split rhythms, after-effects, and motivational interactions. *J. Theor. Biol.* In press.
8. CZEISLER, C. A., E. D. WEITZMAN, M. C. MOORE-EDE, J. C. ZIMMERMAN, AND R. S. KRONAUER. Human sleep: its duration and organization depend on its circadian phase. *Science* 210: 1264-1267, 1980.
9. DAAN, S., AND C. S. PITTENDRIGH. A functional analysis of circadian pacemakers in nocturnal rodents. II. The variability of phase response curves. *J. Comp. Physiol.* 106: 253-266, 1976.
10. DECOURSEY, P. J. Phase control of activity in a rodent. *Cold Spring Harbor Symp. Quant. Biol.* 25: 49-55, 1960.
11. ENRIGHT, J. T. *The Timing of Sleep and Wakefulness*. New York: Springer-Verlag, 1980.
12. GROSSBERG, S. The processing of expected and unexpected events during conditioning and attention: a psychophysiological theory. *Psychol. Rev.* 89: 529-572, 1982.
13. GROSSBERG, S. Some psychophysiological and pharmacological



- correlates of a developmental, cognitive, and motivational theory. In: *Brain and Information: Event Related Potentials*, edited by R. Karrer, J. Cohen, and P. Tueting. New York: NY Acad. Sci., 1984.
14. GROSSBERG, S. Some normal and abnormal behavioral syndromes due to transmitter gating of opponent processes. *Biol. Psychiatry* 19: 1075-1118, 1984.
  15. HODGKIN, A. L. *The Conduction of the Nervous Impulse*. Liverpool: Liverpool Univ., 1964.
  16. HOFFMANN, K. Splitting of the circadian rhythm as a function of light intensity. In: *Biochronometry*, edited by M. Menaker. Washington, DC: Natl. Acad. Sci., 1971, p. 134-150.
  17. INOUE, S. T., AND H. KAWAMURA. Persistence of circadian rhythmicity in a mammalian hypothalamic "island" containing the suprachiasmatic nucleus. *Proc. Natl. Acad. Sci. USA* 76: 5962-5966, 1979.
  18. KRAMM, K. R. *Circadian Activity in the Antelope Ground Squirrel, Ammospermophilus leucurus* (PhD thesis). Irvine, CA: Univ. of California, 1971.
  19. MARTINEZ, J. L. Effects of selected illumination levels on circadian periodicity in the rhesus monkey (*Macaca mulatta*). *J. Interdiscip. Cycle Res.* 1: 47-59, 1972.
  20. MOORE, R. Y., AND V. B. EICHLER. Loss of a circadian adrenal corticosterone rhythm following suprachiasmatic lesions in the rat. *Brain Res.* 42: 201-206, 1972.
  21. OLDS, J. *Drives and Reinforcements: Behavioral Studies of Hypothalamic Functions*. New York: Raven, 1977.
  22. PICKARD, G. E., AND F. W. TUREK. Splitting of the circadian rhythm of activity is abolished by unilateral lesions of the suprachiasmatic nuclei. *Science* 215: 1119-1121, 1982.
  23. PITTENDRIGH, C. S. Circadian rhythms and the circadian organization of living systems. *Cold Spring Harbor Symp. Quant. Biol.* 25: 159-185, 1960.
  24. PITTENDRIGH, C. S., AND S. DAAN. A functional analysis of circadian pacemakers in nocturnal rodents. I. The stability and lability of spontaneous frequency. *J. Comp. Physiol.* 106: 223-252, 1976.
  25. PITTENDRIGH, C. S., AND S. DAAN. A functional analysis of circadian pacemakers in nocturnal rodents. V. Pacemaker structure: a clock for all seasons. *J. Comp. Physiol.* 106: 333-355, 1976.
  26. POHL, H. Characteristics and variability in entrainment of circadian rhythms in light in diurnal rodents. In: *Vertebrate Circadian Systems*, edited by J. Aschoff, S. Daan, and G. A. Groos. New York: Springer-Verlag, 1982, p. 339-346.
  27. ROWSEMITT, C. N., L. J. PETTERBERG, L. E. CLAYPOOL, F. C. HOPPENSTEADT, N. C. NEGUS, AND P. J. BERGER. Photoperiodic induction of diurnal locomotor activity in *Microtus montanus*, the montane vole. *Can. J. Zool.* 60: 2798-2803, 1982.
  28. STEPHAN, F. Y., AND I. ZUCKER. Circadian rhythm in drinking behavior and locomotor activity of rats are eliminated by hypothalamic lesions. *Proc. Natl. Acad. Sci. USA* 69: 1583-1586, 1972.
  29. WEVER, R. A. Autonome circadiane Periodik des Menschen unter dem Einfluss verschiedener Beleuchtungs-Bedingungen. *Pfluegers Arch.* 306: 71-91, 1969.
  30. WEVER R. A. *The Circadian System of Man: Results of Experiments Under Temporal Isolation*. New York: Springer-Verlag, 1979.
  31. YELLIN, A. M., AND G. T. HAUTY. Activity cycles of the rhesus monkey (*Macaca mulatta*) under several experimental conditions, both in isolation and in a group situation. *J. Interdiscip. Cycle Res.* 2: 475-490, 1971.